



10.5281/zenodo.16605

ANALYTICAL AND TECHNOLOGICAL EVALUATION OF ANCIENT LEAD SLAGS FROM LAVRION, ATTIKA, GREECE

C. Tsaimou, P.E. Tsakiridis* and P. Oustadakis

*School of Mining & Metallurgical Engineering, National Technical University of Athens
9 Iroon Polytechniou str., 157 80, Zografou, Athens, Greece*

Received: 25/10/2014

Accepted: 20/04/2015

Corresponding author: P.E. Tsakiridis (ptsakiri@central.ntua.gr)

ABSTRACT

The present research reports the chemical and mineralogical results of various archaeometallurgical lead slags from the Ari site at Lavrion, one of the largest ancient sites of Pb–Ag metallurgical activities in Greece, excavated by the School of Mining and Metallurgical Engineering of Greece, under the directorship of Prof. C. Tsaimou. Dating of the metallurgical slags was carried out using radiocarbon measurements, indicating the earliest phase of the Roman Empire. Chemical analysis, X-ray diffraction (XRD), Fourier transform infrared spectroscopy (FT-IR) and scanning electron microscopy (SEM) were used to identify the Ca-rich silicate, oxides and metallic phases. The major constituents of the slag proved to be melilite (akermanite/hardystonite), clinopyroxene, olivine, spinel and glass. Zinc was dissolved in the silicate melt and was mostly present in the form of the zinc member of the spinel and as silicate (hardystonite). Lead, in contrast, behaves as an “incompatible element” and was likely to be concentrated in the residual matrix. Pb was also present in the form of metallic inclusions.

KEYWORDS: Ancient Pb Slags, Radiocarbon Dating, Mineralogy, Microstructure.

1. INTRODUCTION

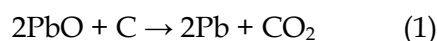
The mining and metallurgical activity developed from Lavreotiki peninsula took place since the Final Neolithic period and it was continued until 20th century. In the Bronze Age (2800-1100 BC), the mines of Lavrion supplied all the great Aegean cultures (Cycladic, Minoan and Mycenaean) with silver, lead and most likely copper (Papadimitriou, 2000). The ancient Greeks exploited the minerals of Lavrion to extract (mainly) silver and lead, with remarkable techniques of underground exploitation, hydrometallurgical processing and smelting of low grade ore deposits (Conophagos, 1980; Papadimitriou, 2000; Kakavoyannis, 2001). The extraction of silver from rich argentiferous lead ores, by cupellation, formed the heart of Lavrian metallurgy and laid the base for Athens economic and cultural wealth and dominance during the classical period. It should be noticed that within the Aegean area, except Lavrion, three other main centers are attested by ancient authors: the island of Siphnos, the island of Thasos and various districts in Macedonia and Thrace. However, the multi-metallic ore deposits of Lavrion were already used in the Early Bronze Age both for copper and silver. As a result, the richest and deepest levels were exploited fully since 480 B.C. (Conophagos, 1980; Gale et al, 1984; Papadimitriou, 2000).

Silver was a valuable commodity in ancient times and until the decline of the Roman Empire, lead was principally obtained as a by-product of silver production. The argentiferous lead ore was melted in furnaces and exposed to a blast of air. Two molten fluids were tapped from the furnace and allowed to solidify. The lead-silver metal alloy, which was the most dense, was settled on the bottom, to be overlain by the slag, a semi-glassy largely silicate material. The silver metal was then separated from the lead by cupellation, a process already ancient in Roman time. The metal was placed in a ceramic bowl (the cupel) in a furnace and a strong blast of air blown across the surface of the molten

metal. The lead oxidized to form PbO (litharge, from Greek for the "spume of silver") and the relatively pure silver remained as metal (Conophagos, 1980; Craddock, 1995).

The litharge produced from the cupellation process could be recycled through the smelting furnace to recover the lead metal (Kuleff et al, 2006; Ferrer-Eres, 2010). There is evidence of lead workings and artefacts from very early periods, in excavations dating well before the time of the Roman Empire. Early Copper Age production of lead was mainly located in Asia Minor. However, later lead production centres emerged in the Aegean and Greece (from 2100-1200 BC) and to the Iberian Peninsula (1200 BC to 500 AD). Lead was used on a large scale especially by Greeks, Carthaginians and Romans, as a useful material in its own right, for alloying, building and a host of miscellaneous uses. The use of lead declined after the collapse of the Roman Empire, but in the Middle Ages in Europe, lead began to be used anew for many applications, including water piping and paints, which have recently been phased out, or at least greatly reduced, in view of the potential for risks to health (Nriagu, 1983).

During the smelting process, lead oxide could be reduced in charcoal or wood fires below 900°C. A series of reactions took place in the furnace, but overall the effect is:



The lead was molten and was tapped off from the bottom of the furnace. The fluxes with gangue formed a molten slag, a material composed of metal oxides and silicates. This process was very simple, but presented the problem of relatively low metal lead recovery. A large quantity of lead was lost to the slag, which was tapped or allowed to flow from the furnaces. This type of smelting slags is well crystallized and presents only a few large gas bubbles. The majority of mineral phases are not 'stoichiometric' chemical compounds present in natural conditions (Bachmann, 1982). Due to their relative fast crystallization process these

mineral phases may be regarded as unstable. The elemental composition of the chemical compounds is usually much different from that of their analogues present in ores.

Rather than a mere waste, slag was a technological by-product intentionally designed to optimize metal yield. The mineral charge was smelted approaching eutectic compositions, namely compositions able to produce low temperature melts. Effective metal-silicate segregation in the furnace was achieved through the design of low viscosity melts. The starting ore, furnace temperature, flux and processing technology are all recorded within the slags.

The density and viscosity of the molten slag had to be kept low enough to ensure the gravity separation of metal-rich liquids, containing elevated amounts of the desired metal. Silicate slag floated on the surface and concentrated the oxide components of the silicate gangue and additives. Slag also contained metal-rich droplets unable to decant in time during the smelting process. In contrast with the other metals, most of zinc was vaporized or dissolved in the liquid silicate slag - up to 20% ZnO (Ettler et al, 2001). The vaporized zinc could subsequently condense, forming oxides trapped by the molten slag.

Most of the slags are dense and dark gray to black and appear stony or visibly crystalline (Navarro et al, 2008; De Caro et al, 2015). The slag generally contains a relatively high amount of lead and most of any zinc present. On the other hand the lead obtained from the above process may contain small amounts of some metallic impurities also contained in the ore. These can include the metals: copper, arsenic, antimony, bismuth, tin and silver. The tracing of these elements, particularly the volatile ones such as arsenic and antimony could serve as ore provenance indicators (Tylecote, 1976; Farquhar et al, 1998; Manasse and Mellini, 2002). It should be noticed that, mineralogically, the furnace by-products of metal smelting show the following primary phases: melilite, spinels, Zn-rich Ca-Fe silicates, Zn-rich fayalite,

metal oxides, metallic Pb and glass (Kucha et al, 1996).

The aim of the present research work is the mineralogical and microstructure examination of archaeometallurgical lead slags from the Ari site at Lavrion, excavated by the School of Mining and Metallurgical Engineering of Greece under the directorship of Prof. C Tsaimou. Chemical analysis, X-Ray diffraction, Fourier transform infra red spectroscopy and scanning electron microscopy were used in order to identify the chemical and mineralogical composition, as well as the microstructure of the selected slag samples.

1.1 Site Location

Ancient metallurgical slags from Ari site, near the Lavrion port, played a key role in the discovery of smelting furnaces and other archaeometallurgical features. Lavrion is located on the southeast tip of the prefecture of Attica, 52 km from Athens. The mining works extend over an area of 120 km from the site of Daskaleio to Cape Sounion and Legrena.

Ari is a valley about 2 kilometers long located at the northwest part of Lavreotiki peninsula, between Anavissos and Keratea towns, approximately 10 km from the city of Lavrion (Figure 1).

Due to its rich ore deposits, the valley is a rare case amongst industrial plants, since ancient industrial facilities coexist with others of modern era. The archaeological excavations revealed a number of cyclic plane sluices (Figure 2), which are part of large complexes for the ore enrichment and framed with flat washeries and many workrooms (Figure 3). The new findings promoted the knowledge of ancient Greek ore enrichment process. The circular marble structures do not fall into the category of helical washery, where ancient miners enriched the poor ore, since they do not form a helix of one coil.

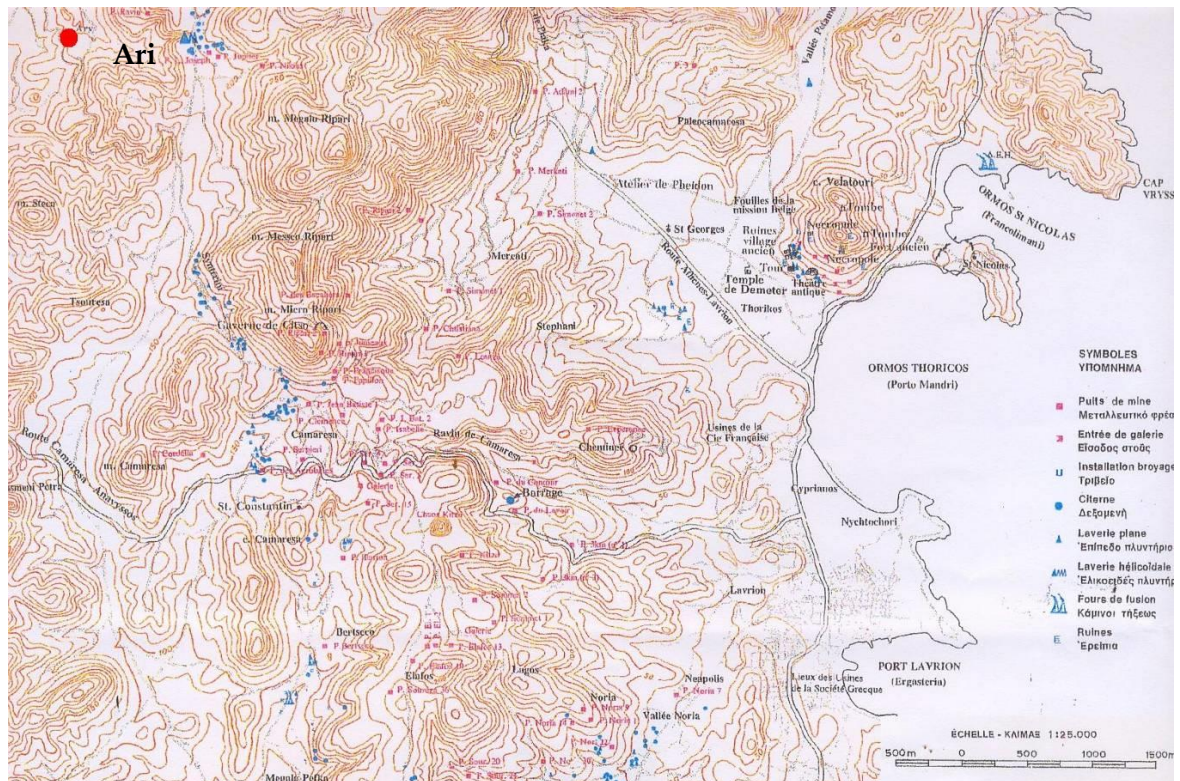


Figure 1 Map showing the location of the Ari site, near at Lavrion port [Conophagos, 1980]



Figure 2 Excavated cyclic plane marble sluice from Ari site, Lavrion.

According to the archaeological findings, these marble cyclic sluices (after the ore grinding and enrichment to the flat washeries) were probably used for ore formation into the eventual shape of briquettes, which were fed to smelting furnaces. The cyclic plane sluices found in Ari (Figure 2) show that the ancient Greeks, apart from the ore enrichment structures (flat and helical washeries), fabricated additional special structures, unknown until today in the

scientific community. The presence of a large workshop with eight smelting furnaces in short distance from a similar circular structure should be also noted (Figure 4). According to the surface finds so far, which include (slags, silver-poor litharge, metallic lead, ceramics) the whole ore enrichment complex in the Ari site has been dated from the 4th century BC (Tsaimou, 2005).



Figure 3 Excavated complex of ore enrichment from Ari site, Lavrion.



Figure 4 Uncovered lead smelting furnaces from Ari site, Lavrion

2. EXPERIMENTAL

Six samples of lead slag (identified as S1 to S6), resulting from the systematic excavation in the Ari site (Lavrion region), were investigated. Their direct dating by radiocarbon measurements was carried out since wood charcoal was the primary fuel source employed for smelting and metalworking. As a result, significant quantities of charcoal fragments have been usually associated with the metallurgical findings. During radiocarbon measurements, both $^{14}\text{C}/^{12}\text{C}$ and $^{13}\text{C}/^{12}\text{C}$ isotopic ratios for each graph-

ite target were determined. Chemistry blank samples for background corrections and standard samples for normalization purposes were also measured. Radiocarbon concentration in measured samples were obtained correcting the measured $^{14}\text{C}/^{12}\text{C}$ isotopic ratios for isotopic fractionation and background, and normalizing them to the isotopic ratios measured for the standards. Radiocarbon ages were converted to calendar ages using the Radiocarbon Calibration Program, version 5.0 (Reimer et al, 2004).

Seven major elements (Si, Pb, Ca, Fe, Zn, Al, Mg,) were determined by atomic ab-

sorption spectrophotometer (Perkin Elmer 4000). The analysis of Pb, Ca, Fe, Zn and Mg was done using air-acetylene flame. In the case of Al and Si, nitrous oxide-acetylene flame was used. Ag, As, K, Na and Mn were determined by inductively coupled plasma mass spectrometry (ICP-MS, X Series II, Thermo Scientific).

X-Ray Diffraction analysis have been conducted with a Bruker D8-Focus diffractometer by a powder diffraction method, with nickel-filtered $\text{CuK}\alpha$ radiation ($=1.5406 \text{ \AA}$), 40 kV voltage and 40 mA current.

Lead slags were also characterized by a Spectrum GX (Perkin Elmer) Fourier transform spectrophotometer, in the range of $4000\text{-}400 \text{ cm}^{-1}$, using the KBr pellet technique. The pellets were prepared by pressing a mixture of the sample and dried KBr (ratio, about 1:200) at 8 tons/cm². The spectrometer was equipped with a deuterated triglycine sulfate (DTGS) detector and with an attenuated total reflectance (ATR) unit. The ATR sampling compartment is a ZnSe crystal (refractive index 2.4) with an angle of incidence of 45° oriented horizontally. The size of the rectangular surface area of the ATR crystal is 60 mm×10 mm.

Finally, the microstructure of the slag samples was evaluated by scanning electron microscopy (SEM) using a Jeol 6380 LV microscope. Experimental conditions involved 15 kV accelerating voltage at low vacuum (30 Pa), using a backscattered electron detector. Microanalysis was performed by an Oxford INCA Energy Dispersive Spectrometer (EDS) connected to the SEM. SEM was performed in polished sections, which were produced by vacuum impregnation, of the selected sample, in a low viscosity epoxy resin. After removing a small surface by cutting in micro-saw, the sample was grinded and polished with 1µm diamond paste, on a lapping disk.

3. RESULTS & DISCUSSION

3.1 Macroscopic Characteristics-Dating

A total of six samples of lead slag, the waste product of smelting incorporating most of the unwanted elements in the ores, were examined. According to the ceramic typology of the archaeometallurgical finds and the radiocarbon analysis, the slags are dated from the 2nd -1st centuries BC, in other words the earliest phase of the Roman Empire (Table 1).

Table 1: Results of radiocarbon dating of charcoal samples

Sample Material	¹⁴ C Date yr (BP)	$\delta^{13}\text{C}$ (%)	Calibrated Age	Probability (%)
Charcoal	2110 ± 30	-22.99	203-46 BC	95.4
Charcoal	2101 ± 30	-24.55	198-47 BC	95.4



Figure 5 Slag fragments from the Ari site, Lavrion.

All samples consisted of pieces 5-15 cm thick with wrinkled or bubble-pocked up-

per surfaces. The textural features of the slags depend upon the cooling rates. They are well crystallized and show only a few large gas bubbles. They are all grey-black in color (Figure 5) and contain small metallic inclusions of Pb visible in their matrix.

3.2 Chemical Composition

The chemical composition of the examined slags is reported in Table 2. The slags were composed of up to 65% SiO_2 , CaO, Fe_2O_3 and Al_2O_3 and up to 35% PbO and

ZnO. The measurements showed that silica (24-26%) and lead oxide (20-22%) are the main constituents, followed by calcium oxide (13-16%) and iron oxide (10-18 %) and smaller amounts of other gangue elements.

Table 2: Chemical Analysis of Slags

(% wt)	S1	S2	S3	S4	S5	S6
Si	12.18	12.21	11.38	11.36	11.55	11.87
Ca	11.13	11.09	11.56	10.11	9.69	9.51
Al	2.49	2.46	2.43	1.6	2.45	2.33
Fe	9.89	10.84	11.92	7.13	8.09	13.11
Mg	1.48	1.87	1.37	1.23	1.72	1.73
K	0.97	0.95	0.86	0.66	1.01	1.08
Na	0.45	0.4	0.35	0.3	0.45	0.4
Zn	7.44	8.1	7.46	17.67	14.85	7.78
Pb	20.84	18.86	19.67	18.09	17.16	18.53
Mn	0.51	0.81	0.82	0.9	0.92	0.9
Ag	0.0015	0.0003	0.0008	0.0007	0.0004	0.0006
As	0.19	0.07	0.08	0.97	0.05	0.05

According to the results, it is about Ca-rich silicate slags, which floated on the surface and concentrated the oxide components of the silicate gangue and additives. Lead, which was present mostly as metal-rich droplets of Pb, was unable to decant in time during the smelting process. Its high content confirmed the relatively low metal lead recovery, which is characteristic of ancient smelting process. Except lead, all slags contain 7-15% ZnO, 0.05-0.19% arsenic and 0.0003-0.0015% Ag. The low content of silver is a strong indication that the slags are coming rather from the production of lead than from a primary silver production. The presence of arsenic and zinc, which derived from the initial ore, is an indication of using the barren ore (after the ore enrichment in previous stages for silver recovery), not only as a raw material, but as a flux as well, for the formation of the molten slag (Conophagos, 1980; Papadimitriou, 2000; Kuleff et al, 2006). Much of the arsenic must have been vaporized in the smelting process, hence there is relatively little in the furnace products, whereas most of the Zn was dissolved and remained in the liquid silicate slag.

Minor elements included MgO, MnO, K₂O and Na₂O. The total of the chemical analyses is below 100%, which has to be attributed to the presence of oxides in the slag. Parts the metals such as Pb were present in the oxidic state and sometimes FeO can be present in the trivalent and MnO in its tri- or tetravalent form. Slags contain quantities of iron oxide which depends on variables such as the temperature and atmosphere inside the furnace, as well as on the quality of the ore used and the presence of additional ingredients such as silica and lime.

3.3 Characterization by X-ray Diffraction

The X-ray diffraction spectra of the examined slags from Ari site in Lavrion are given in Figure 6. They are composed essentially of CaO rich silicate (melilite group and clinopyroxene), olivines, oxides (spinel), metallic phases and glass. Akermanite (Ca₂MgSi₂O₇) and hardystonite (Ca₂ZnSi₂O₇) are the predominant phases. They belong mineralogically to a complex solid solution with the general formula X₂YZ₂O₇ or (Ca,Na,K)₂(Mg,Fe²⁺,Fe³⁺,Al)(Si,Al)₂O₇ (Deer et al, 1992). In iron-rich silicate slag produced by the old iron metal-

lurgy, melilite group phases normally occurs only as an accessory constituent. Meli-

lite is usually the main component in the Ca-Mg slags (Ettler et al, 2000).

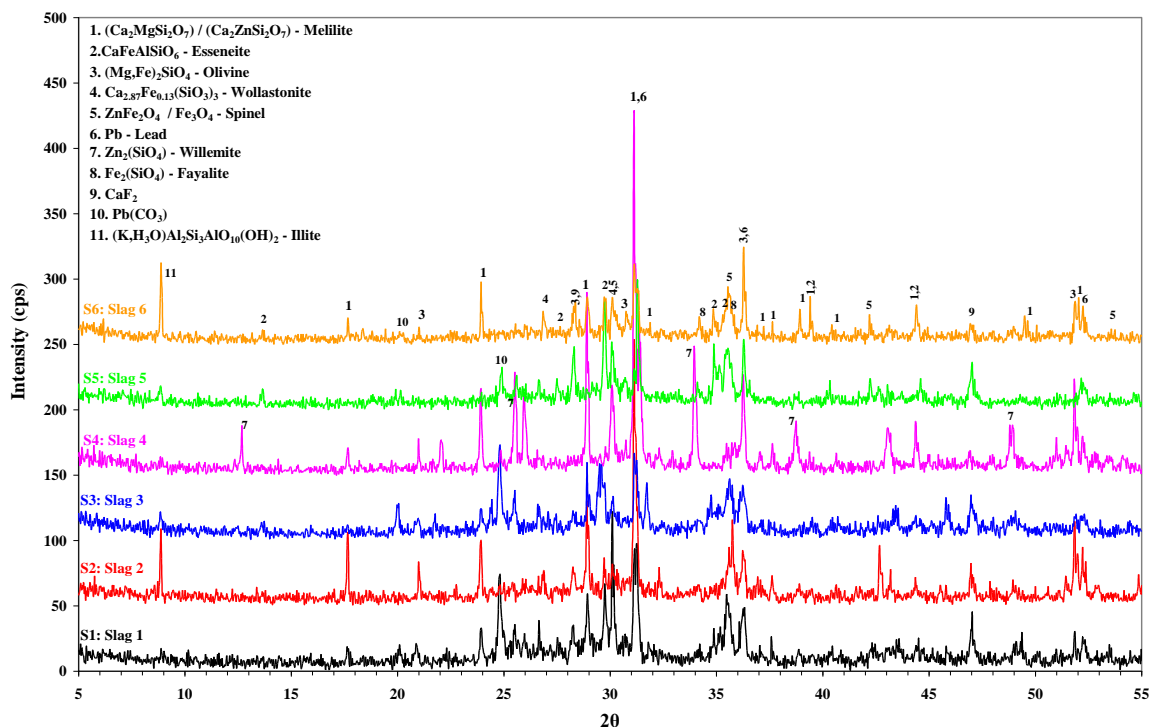


Figure 6 X-Ray Diffraction patterns of the examined slags from Ari Site, Lavrion.

The detection of ZnFe_2O_3 (zinc ferrite), except Fe_3O_4 , indicates that the trivalent iron was able to combine with zinc to produce the spinel phase upon cooling from the melt. In contrast with the other metals, most of the Zn is vaporized or dissolved in the liquid silicate slag. The vaporized Zn can subsequently condense, forming mixed oxides trapped by molten slag. During the cooling of the melt, zinc enters first into the spinel structure. Melilite starts to nucleate simultaneously with spinel and also concentrates Zn (Saffarzadeh et al, 2006).

Phase occurrence largely depends on chemical composition. For instance, the detection of calcic clinopyroxenes esseneite (CaFeAlSiO_6) indicates Ca-rich slags. Esseneite usually occurs with anorthite or melilite solid solutions and glass. The formation of olivine is due to the presence of magnesium oxide in the slag. The dissolution of MgO into most slags usually results in increasing the liquidus temperature of the slag with respect to an MgO containing phase such as magnesia wustite, spinel or

olivine phase. It should be noticed that slags with lower Mg content would crystallize only pyroxenes instead of olivine (Devic and Marceta, 2007).

The strong peak of metal Pb confirms the fact that because of the smelting process, large quantity of lead was lost to the slag, which was allowed to flow from the furnaces and to solidify. The occurrence of a small amount of glassy phase (slow rate of cooling) is denoted by the small background and particularly by the characteristic small hump in the 25° 2θ and 35° 2θ range of the diffraction pattern.

Wollastonite ($\text{Ca}_{2.87}\text{Fe}_{0.13}(\text{SiO}_3)_3$) has been probably stabilized by the presence of impurity ions (Fe^{3+} , Al^{3+}) and relatively slow rate of cooling. Fayalite (Fe_2SiO_4) was also detected in all slags at lower percentages. However, the predominance of zinc ferrite and magnetite indicates only slightly reducing conditions, while the presence of fayalite together with the samples heterogeneity show that the operating conditions

are likely to have fluctuated considerably during the process (Kucha et al, 1996).

It should be noticed the detection of the Zn-bearing fayalite (Zn_2SiO_4) in slags S4 and S5. Zn substitutes for Fe^{2+} in the fayalite crystal structure. Zn enters into the crystal structures of oxides and silicates (spinel, melilite, clinopyroxene and olivine), due to the substitution for Fe^{2+} in octahedral sites (Ericsson and Filippidis, 1986).

It is likely that CaF_2 is relic of the primary ore, while the presence of small amount of cerrusite should be attributed to the partial carbonation of PbO content in slags (hydration-carbonation cycles). The occurrence of illite ($(K,H_3O)Al_2Si_3Al O_{10}(OH)_2$) is

due to the sampling procedure, where clay minerals were not fully removed from the slags samples. A minor amount of quartz is also present.

3.4 Characterization by FT-IR

Infrared absorption spectra of crystalline substances gave valuable information on the slag samples structure and supplied conclusive evidence on the nature of the functional groups present in the crystal lattice. The FT-IR spectra of the examined slags (Figure 7) identify silicates as the most abundant components.

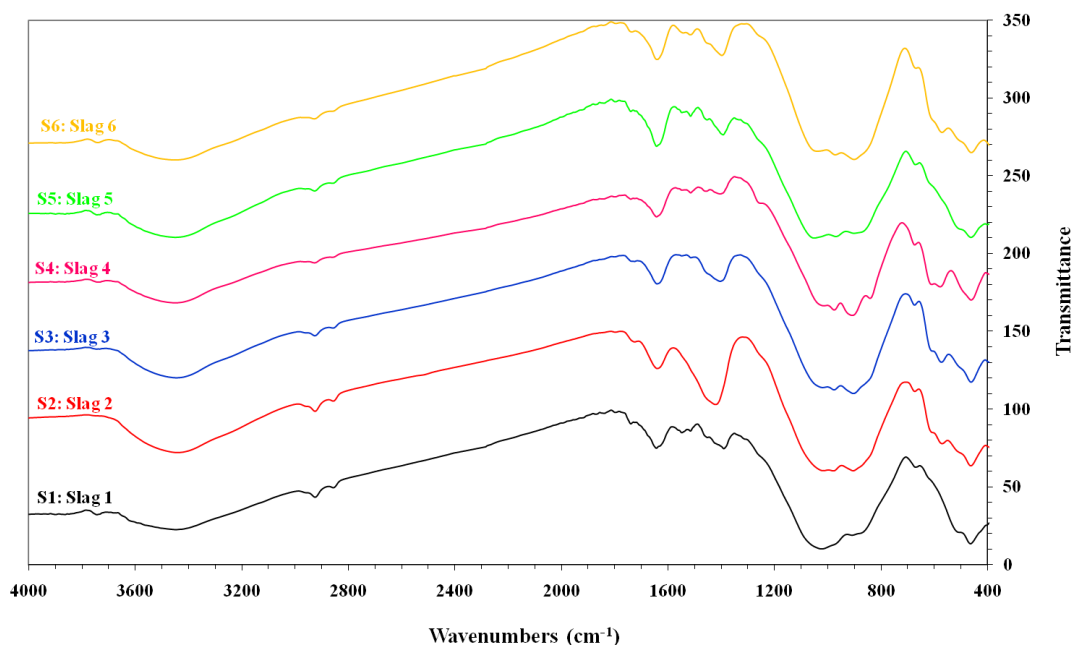


Figure 7 FT-IR spectra of the examined slags from Ari Site, Lavrion

The 850-1000 cm^{-1} region may be attributed to the Si-O stretching absorption in O-Si-(OCa) of calcium silicate, the 1000-1080 cm^{-1} region to that of O-Si-(OAl) of aluminosilicate and the 1080-1250 cm^{-1} region to that of O-Si(OSi) or silica. Al-O bonds present with Si-O give vibration peaks of 462 and 523 cm^{-1} . The spectra of all slags exhibit four relative broad transmittance bands in the region of 400-1500 cm^{-1} . This lack of sharp features is indicative of a relative disorder in the silicate network. The absorptions with maxima at 1050, 955, 900 and 860 cm^{-1} are characteristics of Si-O

stretching modes of silica and silicates and correspond to $[SiO_4]^{4-}$ -tetrahedra. The peak position at around 1050 cm^{-1} shifts toward lower wavenumbers with increasing Pb/Si ratio, indicating that Pb is incorporated into the glassy matrix.

The composition of melilite varies significantly and often corresponds to a solid solution of åkermanite ($CaMgSi_2O_7$) and hardystonite ($CaZnSi_2O_7$) and they are formed due to thermal reaction of the calcite decomposition products with the fired clay. The calcium silicate band intensities correlate well with the calcium content in the

matrix. Their IR absorption were detected at 1050, 935, 900, 849, 720 cm^{-1} . The calcium silicate band of S3 slag is the strongest among the spectra, because the matrix in this sample has the highest calcium, whereas the calcium silicate band of S6 is the weakest (lowest calcium content).

FTIR spectra confirmed the formation of spinel (zinc-ferrite). In FTIR spectroscopy of metal oxides, two ranges of the absorption bands, 400–450 cm^{-1} and 500–650 cm^{-1} , are observed. The high frequency band 550 cm^{-1} is due to the vibration of the tetrahedral M-O bond and the low frequency band 460 cm^{-1} is due to the vibration of the octahedral M-O bond in the crystal lattices of the ZnFeO_4 . The high-frequency band (M-O stretching) shifts to lower energies (from 600 to 550 cm^{-1}) as the Zn occupation of octahedral sites in the spinel structure increases, substituting Fe^{2+} ions.

The weak bands with maximum at 3440 cm^{-1} and 1645 cm^{-1} , which are assigned to O-H stretching and H-O-H bending modes of vibration (ν_2), can be attributed to the absorbed water due to the partial hydration of slag phases. The band centered at 1070–1080 cm^{-1} and the shoulder at 980 cm^{-1} are the symmetrical vibration of $(\text{SO}_4)^{2-}$. A doublet is also observed near 600 and 670 cm^{-1} due to the ν_4 $(\text{SO}_4)^{2-}$ bending vibrations. The weak band at 1470 cm^{-1} confirmed the small presence of carbonate species in the samples.

3.5 Microstructure Observations by SEM

All slags fragments were subjected to scanning electron microscopy (SEM) using a backscatter detector, in conjunction with energy dispersive spectroscopy (EDS). The minerals crystallization is the result of the smelting process and always are euhedral fully developed crystals or skeletal crystals with hopper structures. Sizable euhedral crystals and elongate laths and prismatic crystals are typical for the silicate phases. Rectangular and trellis patterns and isolated octahedra or cubic forms are typical of the oxide phases. Within the isotropic glasses, complex silicate crystalline phases

are the most abundant and oxide crystalline phases are less common (Figures 8,9).

Microscopic examination showed that åkermanite ($\text{Ca}_2\text{MgSi}_2\text{O}_7$) and hardystonite ($\text{Ca}_2\text{ZnSi}_2\text{O}_7$), of the melilite group, are the most abundant crystalline phase in all slags and are crystallized with the form of planar slabs. Melilite-type phases crystallize only in Ca-rich melts and form in both slowly cooled and quenched slag.

Zinc ferrite and magnetite (spinel) developed through crystallization from the melt into idiomorphic individuals, but exists also in eutectic growth with melilite phases. The spinel-group phase is amongst the first to crystallize from the silicate melt. While the silicates nucleate simultaneously with the oxides, small crystals of spinel appeared to be embedded in melilite phase. The magnetite and zinc ferrite spinel oxides occur in all of the slags and appear most frequently as cubic to octahedral euhedral crystals. Sometimes spinel crystals exhibited skeletal form, where the cores are hollow. In back-scattered electron mode, the zinc ferrite grains presented an optical zoning, with a bright core and a significantly darker grey rim. The brighter internal parts are enriched in Zn, and the darker external parts are Fe-rich.

All slags from Ari site in Lavrion contained clinopyroxene, due to their high CaO-content. A precondition for the crystallization of an iron-rich pyroxene is the existence of CaO, because ferrosilite (FeSiO_3) is not stable. Clinopyroxene was detected with the form of euhedral prismatic long crystals. EDS analysis proved that it was actually a Ca-Fe-Al clinopyroxene, which was detected as esseneite (CaFeAlSiO_6) by X-ray diffraction. Its crystal size, as well as that of the melilite (the two dominant phases in all slags), indicates a relatively slow cooling rate (Ettler et al, 2009). The amount of Zn bound in clinopyroxene occurring was low (1.5 wt.% ZnO), suggesting that the clinopyroxene could not accommodate more Zn under the conditions of its crystallization.

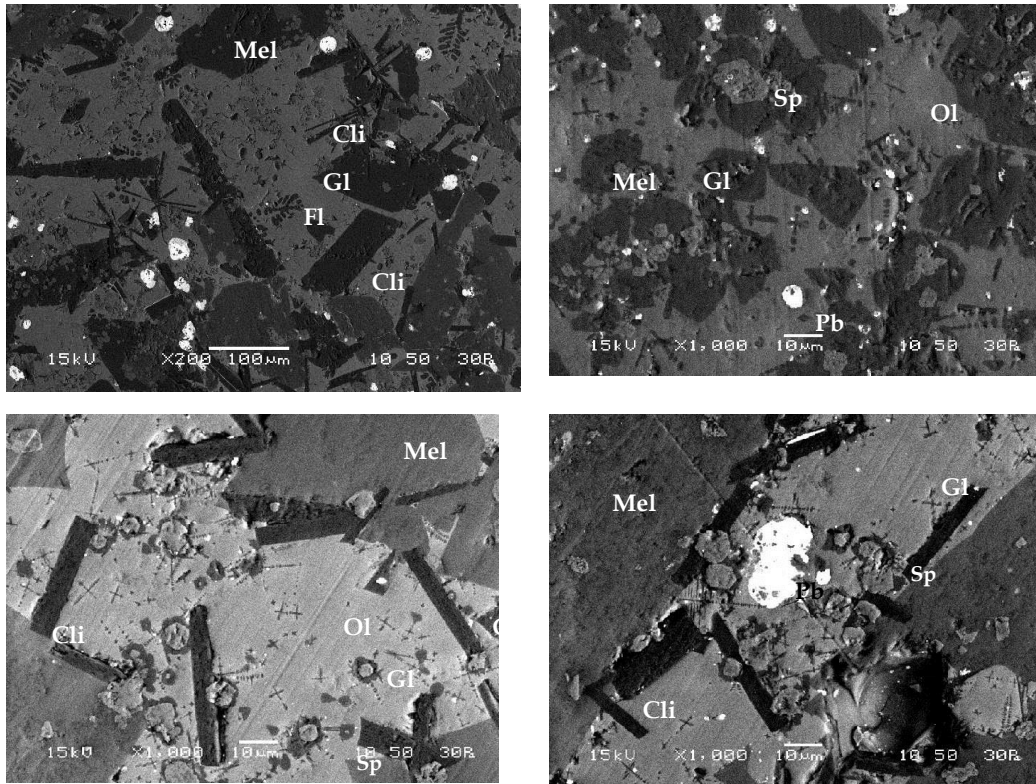


Figure 8 Prismatic crystals of melilite (Mel) and columnar clinopyroxene (Cli). Euhedral crystals of spinel (Sp) embedded in glassy matrix (Gl) and in eutectic growth with melilite (dark area around spinel grains). Dendritic olivine-group crystals (Ol) in the amorphous glass (Gl) phase. Spherules composed of lead (Pb). Distinct particles of fluorite (Fl) dispersed in matrix

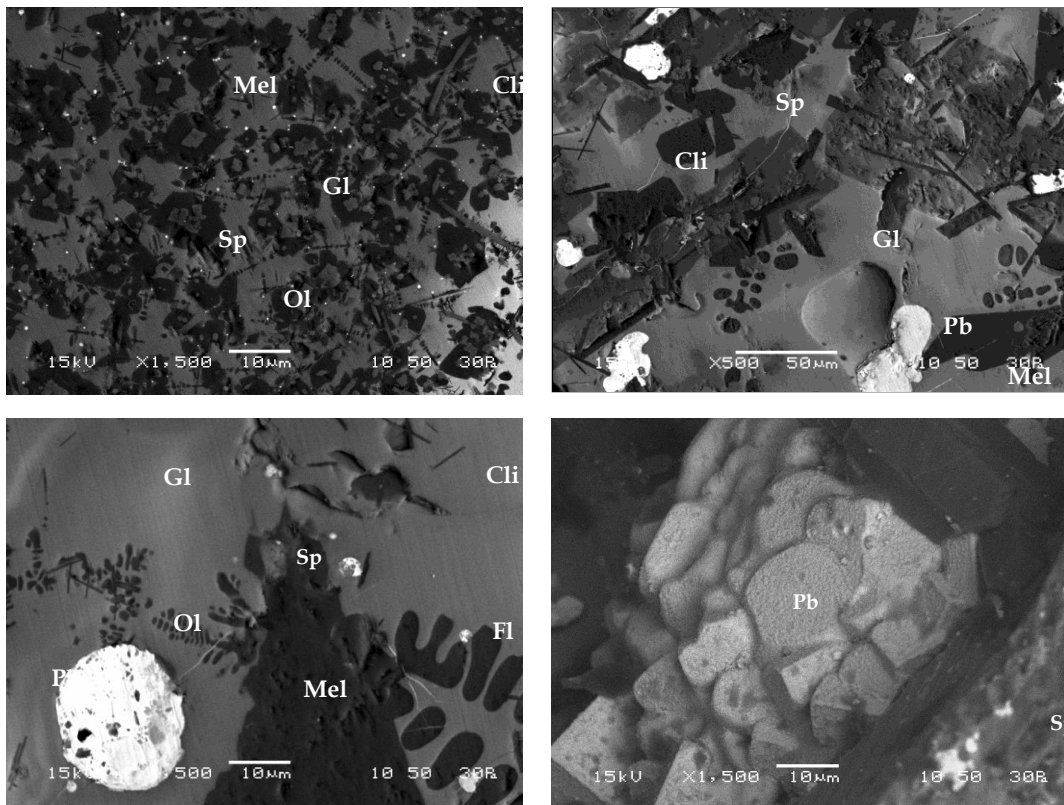


Figure 9 Crystals of spinel (Sp) in eutectic growth with melilite (dark area around spinel grains). Elongate crystals of clinopyroxene and coarse-grained crystals of melilite (Mel). Dendrites of olivine (Ol). Metallic lead inside large pore (Pb).

Sizable euhedral crystals of ferroan wolastonite were detected in all slags. They were typically embedded in glass with higher silica content. Their precise determination was made possible by interpreting the X-ray diffraction pattern and EDS analysis

Olivine-group phases, which represent an isomorphous mixture of forsterite Mg_2SiO_4 and fayalite Fe_2SiO_4 , probably are the last silicates crystallizing from the liquid in all slags, filling spaces between the earlier-crystallized silicates. They form small needles or dendrites, often difficult to analyze by EDS, due to their size. Sometimes, are detected with the form of skeletal crystals, which appear to have crystallized directly from the host melt. In slags S4 and S5, olivine's chemical composition corresponds to Zn_2SiO_4 (willemite). Its presence support the suggestion that Zn (ionic radius 0.74 Å) can enter into octahedral sites of the structure and substitute for Fe^{2+} (ionic radius 0.76 Å) (Ericsson and Filippidis, 1986).

The glass phase is usually found colorless but in places it has light brown to yellow in colour and typically contains complex silicate mineral phases. It is chemically heterogeneous and it is formed mostly by silicon, calcium, iron, aluminum and magnesium. It also exhibits elevated concentrations of Zn, whereas in comparison with the crystalline silicates, it presents higher percentages of Pb.

Pb metallic phases are easy to distinguish in the material due to their characteristic reflectance when compared with the other ore minerals. They have various complicated forms: drop-like, vermicular and oval. Pb behaves as incompatible element since it has been markedly characterized as part of polymetallic alloys in the form of spherical metallic inclusions associated with other trace elements such as Sb, Sn, As, Zn and Al. samples.

3.6 Crystallization Process

The crystallization process of the slags is a heterogeneous transformation and as such consists of two stages, namely a nu-

cleation stage and a growth stage. In the nucleation stage small, stable volumes of the crystalline phase are formed, usually at preferred sites in the parent glass phase (Rawlings et al, 2006). Once a stable nucleus has been formed the crystal growth stage commences. Growth involves the movement of atoms/molecules from the glass phase, across the glass-crystal interface, and into the crystal.

The smelting process was taken place in blast furnaces, where lead phases could be reduced with charcoal or wood fires. The raw material was charged with limestone flux and/or the poor barren lead ores (which also contained small quantities of $PbCO_3$) and other additives, such as silica or iron oxide (Conophagos, 1980). The use of the barren ore was also confirmed and by the presence of CaF_2 and $BaSO_4$ in the slag, which derived from the primary ore. The fluxes helped to the formation of the molten slag (oxides/silicates).

The dominant part of the examined slags from Ari site at Lavrion, mostly consists of grains of silicates and spinels, as well as subordinate amounts of other phases. The crystal size of the two silicates dominant phases (melilite, clinopyroxene) indicates a relatively slow rate of crystallization. The proposed crystallization path for the examined slags is: spinel /melilite /clinopyroxene /olivine /glass. The presence of Ca-rich silicates in all slag fragments suggests the presence of $CaCO_3$ in the melting agent (flux).

As was mentioned above, spinel was the first to crystallize from the melt. The zinc and iron minerals are oxidised to ZnO and Fe_2O_3 , respectively, forming magnetite and zinc ferrite crystals. The trivalent iron is able to combine with zinc to produce the spinel phase upon cooling from the melt. Because of the high CaO content in the slag, melilite starts to nucleate almost simultaneously with spinel. While melilite nucleate simultaneously with the oxides, it usually encloses small crystals of spinel. As crystallization of the silicate melt proceeds, zinc which is dissolved in the silicate melt is partially incorporated into the structure

of the melilite phases, forming hardystonite ($\text{Ca}_2\text{ZnSi}_2\text{O}_7$). The zinc content in spinel and melilite phases indicates that the slag crystallization took place under “zinc-saturated” conditions.

The formation of the clinopyroxene constitutes the most complex system during slag crystallization. That formation depends on temperature and the concentration of alumina, silica, iron oxide and lime. It must be pointed out that prior to melting, the system was highly heterogeneous. The slow rate of cooling inside the slag fragments allowed clinopyroxene crystallization, following the reaction of calcium oxide with the aluminosilicates from the melted vitreous matrix.

Olivine phases are late in the crystallization sequence, probably owing to their Mg-poor compositions. The presence of Fe_2SiO_4 (fayalite) and Zn_2SiO_4 (willemite) should be attributed to the partial conversion of the spinel oxides (Zinc ferrite, magnetite) into olivine. These oxides react with the silica to form a molten slag that can be regarded as a mixed solution of Zn_2SiO_4 and Fe_2SiO_4 .

4. CONCLUSIONS

According to the results presented in this paper, the following noteworthy conclusions have been reached:

- All the examined lead slags were compositionally similar and produced by similar smelting technology. Their composition is characterized by relatively low contents of silica and high contents of the divalent cations. The lead concentration ranges from 17 to 21%, confirming that during the smelting process, large quantities of lead were lost to the slag. Furthermore, the very low silver concentration (0.0003-0.0015%) is a strong indication that the slags are coming from the production of lead and not from primary silver production.
- Primary slag phases include: melilite-group minerals (åkermanite - $\text{Ca}_2\text{MgSi}_2\text{O}_7$ and hardystonite- $\text{Ca}_2\text{ZnSi}_2\text{O}_7$), spinel-

group minerals (magnetite- Fe_3O_4 and zinc ferrite- ZnFe_2O_3), clinopyroxene (eseneite- CaFeAlSiO_6), olivine-group minerals (olivine- $(\text{Mg,Fe})_2\text{SiO}_4$, fayalite- Fe_2SiO_4 and willemite- Zn_2SiO_4) and glass.

- The presence of Ca-rich silicates (melilite, clinopyroxene,) in all slags indicates the presence of CaCO_3 or lime, being used as melting agents. The presence of CaF_2 and BaSO_4 in all samples, which are derived from the primary ore, indicates and use of the barren local ore (from the ore enrichment stage) not only as a raw material, but also as a flux, for the formation of the molten slag.
- The crystal size of the melilite and clinopyroxene (the two dominant phases in all slags) reveals a relatively slow cooling rate of the initial slag melt. This was further confirmed and by the occurrence of a small amount of glassy phase in the $25^\circ 2\theta$ and $35^\circ 2\theta$ range of the X-ray diffraction pattern, which is denoted by the small background and particularly by the characteristic small hump.
- The slag was rich in zinc, which probably derived from the local ore and it was in its majority dissolved in the silicate melt. During the cooling of the melt, Zn entered into the spinel and melilite structure. On the contrary, Pb was mainly concentrated in the residual glass and Pb-rich metallic inclusions trapped in the glass.
- The surface finds (slags, silver-poor litharge, metallic lead), the old smelting blast furnaces and the low silver content in slags, indicate a primary smelting workshop, where local metallurgists produced metallic lead, using carbon (coke), as both a reducing agent and a source of heat. According to the ceramic typology and radiocarbon analysis the above pyrometallurgical procedures were dated to 2nd -1st centuries BC, in other words the earliest phase of the Roman Empire.

REFERENCES

- Bachmann, H.G., (1982) Archaeometallurgical investigations of ancient silver smelting at Laurion, *Erzmetall: Journal for Exploration, Mining and Metallurgy*, Volume 35, Issue 5, (1982), pp. 246-251.
- Conophagos, C., (1980) The ancient Lavrion and the Greek technique of the silver production, Edition of Greek Company of Editions, Athens (1980), 458 p. (In Greek).
- Craddock, P.T., (1995) Early metal mining and production, Smithsonian Institution Press, New York (1995), 363 p.
- De Caro, T. Riccucci, C., Parisi, E.I., Faraldi, F., Caschera, D., (2015) Ancient silver extraction in the Montevecchio mine basin (Sardinia, Italy): Micro-chemical study of pyrometallurgical materials, *Applied Physics A: Materials Science and Processing*, Volume 113, Issue 4 (2013), Pages 945-957
- Deer, W.A., Howie, R.A., Zussman, J., (1992) *An Introduction to the Rock-Forming Minerals*, 2nd ed. Longman Group UK Limited, Essex, England (1992), p. 696.
- Devic, S., Marceta, L., (2007) Differences in Morphological Properties between the olivine group minerals formed in natural and industrial process, *Journal of Mining and Metallurgy*, 43 B (2007), pp: 99 - 105.
- Ericsson, T., Filippidis, A., (1986) Cation ordering in the limited solid solution $\text{Fe}_2\text{SiO}_4\text{-Zn}_2\text{SiO}_4$, *Am. Mineral.* 71 (1986), pp: 1502-1509.
- Ettler, V., Johan, Z., Touray, J.C., Jelínek E., (2000) Zinc partitioning between glass and silicate phases in historical and modern lead-zinc metallurgical slags from the Příbram district, Czech Republic, *Comptes Rendus de l'Académie des Sciences - Series IIA - Earth and Planetary Science*, Volume 331, Issue 4 (2000), pp: 245-250.
- Ettler, V., Legendre, O., Bodéan, F., Touray, J.C., (2001) Primary phases and natural weathering of old lead-zinc pyrometallurgical slag from Příbram, Czech Republic, *Canadian Mineralogist*, Volume 39, Issue 3 (2002), pp. 873-888.
- Ettler, V., Cervinka, R., Johan, Z., (2009) Mineralogy of medieval slags from lead and silver smelting (Bohutín, Příbram district, Czech Republic): Towards estimation of historical smelting conditions, *Archaeometry*, Volume 51, Issue 6 (2009), pp. 987-1007
- Farquhar, R.M., Walthall, J.A., Hancock, R.G.V., (1995) 18th century lead smelting in central north America: Evidence from lead isotope and INAA measurements, *Journal of Archaeological Science*, Volume 22, Issue 5 (1995), pp: 639-648.
- Ferrer-Eres M.A., Peris-Vicente J., Valle-Algarra F.M., Gimeno-Adelantado J.V., Sánchez-Ramos S., Soriano-Piñol M.D., (2010) Archaeopolymetallurgical study of materials from an Iberian culture site in Spain by scanning electron microscopy with X-ray microanalysis, chemometrics and image analysis, *Microchemical*, Volume 95, Issue 2 (2010), pp. 298-305
- Kakavoyannis, E., (2001) The Silver Ore-Processing Workshops of the Lavrion Region, *The Annual of the British School at Athens*, Volume 96 (2001), pp. 365-380.
- Kucha, H., Martens, A., Ottenburgs, R., De Vos, W., Viaene, W., (1996) Primary minerals of Zn-Pb mining and metallurgical dumps and their environmental behavior at Plombières- Belgium, *Envir. Geol.* 27 (1996), pp:1-15.
- Kuleff, I., Iliev, I., Pernicka, E., Gergova, D., (2006) Chemical and lead isotope compositions of lead artefacts from ancient Thracia (Bulgaria), *Journal of Cultural Heritage*, Volume 7, Issue 4 (2006), pp. 244-256.
- Manasse, A., Mellini, M., (2002) Chemical and textural characterisation of medieval slags from the Massa Marittima smelting sites (Tuscany, Italy), *Journal of Cultural Heritage*, Volume 3, Issue 3 (2002), pp: 187-198.

- Navarro, A., Cardellach, E., Mendoza, J.L., Corbella, M., Domènech, L.M., (2008) Metal mobilization from base-metal smelting slag dumps in Sierra Almagrera (Almería, Spain), *Applied Geochemistry*, Volume 23, Issue 4 (2008), pp: 895-913.
- Nriagu, J.O., (1983) *Lead and Lead Poisoning in Antiquity*, New York (1983), John Wiley and Sons, 437p.
- Papadimitriou, G., (2000) Mining and Metallurgical Activities in Ancient Laurium and its impact on the Golden Era of Athens, Invited Lecture, 5th International Mining History Congress, Milos Island (2000), pp: 33-44.
- Rawlings, R.D., Wu, J.P., Boccaccini, A.R., (2006). Glass-ceramics: Their production from wastes-A Review, *Journal of Materials Science*, Volume 41, Issue 3 (2006) pp. 733-761.
- Reimer, P.J., Baillie, M.G.L., Bard, E., Bayliss, A., Beck, J.W., Bertrand, C.J.H., Blackwell, P.G., Buck, C.E., Burr, G.S., Cutler, K.B., Damon, P.E., Edwards, R.L., Fairbanks, R.G., Friedrich, M., Guilderson, T.P., Hogg, A.G., Hughen, K.A., Kromer, B., McCormac, G., Manning, S., Ramsey, C.B., Reimer, R.W., Remmele, S., Southon, J.R., Stuiver, M., Talamo, S., Taylor, F.W., van der Plicht, J., Weyhenmeyer, C.E., (2004) IntCal04 Terrestrial radiocarbon age calibration, 0-26 ka BP, *Radiocarbon*, Volume 46, Issue 3 (2004), pp.1029-1058.
- Saffarzadeh, A., Shimaoka, T., Motomura, Y., Watanabe, K., (2006) Chemical and mineralogical evaluation of slag products derived from the pyrolysis/melting treatment of MSW, *Waste Management*, Volume 26, Issue 12 (2006), pp: 1443-1452.
- Stos-Gale, Z.A., Gale, N.H., Gilmore, G.R., (1984) Early Bronze Age Trojan metal sources and Anatolians in the Cyclades, *Oxford Journal of Archaeology*, Volume 3, Issues 3 (1984), pp. 23-43.
- Tsaimou, C.G., (2005) The cyclic plane sluices for the ore mineral processing in Ari site of Lavreotiki, *Mineral Wealth*, Volume 137 (2005), pp. 19-28 (in Greek).
- Tylecote, R.F., (1976) *A History of Metallurgy*, 2nd ed. (Institute of Materials/ Bath Press, Avon, 1976)